Radiative Recombination in Highly Excited CdS†

CLAUDE BENOIT À LA GUILLAUME, JEAN-MARIE DEBEVER, AND FRANK SALVAN

*Laboratoire de Physique des Solides associé au Centre National de la Recherche Scientifique,
Ecole Normale Supérieure, Paris, France*

The processes involved in the laser effect in CdS excited by electron bombardment have been studied with the aid of an experimental technique allowing the spectral dependence of the optical gain to be obtained. It is shown that at least three different processes can lead to a laser effect in CdS. The first, which corresponds to a low gain, is due to the annihilation of a free exciton with the emission of a photon and an LO phonon. The second, yielding a medium gain, is due to an exciton-exciton interaction; and the third, which results in a high gain, involves an exciton-electron interaction. These last two processes have been studied theoretically, and the results are compared with the experimental data.

I. INTRODUCTION

A LASER effect in CdS due to electron bombardment was reported in 1964 by Basov,[1] and then by ourselves[2] and Hurwitz.[3] In order to explain these results, we have proposed in another publication[4] a mechanism based on the annihilation of an exciton bound to a neutral acceptor with emission of acoustical phonons, but later it appeared that this interpretation was erroneous. The annihilation of a free exciton with emission of an LO phonon has been considered by Kulewsky and Prokhorov.[5] However, this last process which we have clearly studied, explains only a small part of the observed effects.

All these experiments only study the laser emission spectrum, and this is not sufficient to discover the processes capable of providing gain. We describe here a technique which allows us to record simultaneously the spontaneous emission spectrum and the stimulated emission spectrum corresponding to a given excitation. From the comparison of these two spectra it is easy to deduce the absolute value of the optical gain.

From the experimental results reported here, it is possible to show that at least three different processes can lead to the laser effect in CdS. The first one, which corresponds to a weak gain, is due to the annihilation of a free exciton with emission of a photon and an LO phonon. The second one, corresponding to a medium gain, is based on the exciton-exciton interaction, and the third one, yielding a high gain, is caused by an exciton-electron interaction.

Section II refers to the experimental setup. In Sec.

III, the method of measuring the optical gain is described; and we present in Sec. IV the experimental results relative to the spontaneous emission at small and high excitations, as well as the results related to the optical gain. In Sec. V, we discuss the theory of exciton-LO phonon coupling, and the exciton-exciton and exciton-electron interaction processes. Finally, we compare the theoretical and experimental results.

II. EXPERIMENTAL SETUP

The experimental setup has been described previously,[4] but we want to point out some modifications which have been made.

(i) The current pulse risetime was improved, so that it is now between 0.5 and 1 nsec and the pulse width can be varied from 10 nsec to 1 μsec. The current intensity can reach 20 mA with a focalization diameter on the sample smaller than $500\,\mu$. This corresponds to a maximum current density equal to about 10 A/cm². The electron energy is 25 kV.

(ii) The height of the entrance slit of the spectrometer has been limited to $300\,\mu$. Its width is usually $50\,\mu$ so that the resolution is equal to 5000. A spherical mirror whose center is located near the CdS emitting point, provides the entrance-slit image. This apparatus allows the exploration of an emitting zone of the sample, whose dimensions are equal to those of the entrance slit. It is therefore possible to separate entirely the light emitted by two points on the sample whose distance is greater than $300\,\mu$.

(iii) The recombination light has been studied in two different ways. In the first method, it is analyzed by means of a spectrometer followed by a photomultiplier (whose risetime is 3 nsec) and by a sampling oscilloscope. In the second method, the emitted radiation is directly detected by a rapid vacuum cell followed by a sampling oscilloscope. In this case, the total risetime is equal to 0.3 nsec. It is therefore possible to record the emission spectrum by fixing the gate of the sampling unit at a given time after the beginning of the pulse, so that a "time" description of the phenomenon can be obtained by varying the position of this gate along the pulse.

† This paper is based on a part of the "Doctorat d'Etat" thesis to be submitted by J. M. Debever at the University of Paris.

[1] N. G. Basov, O. V. Bogdankevich, and A. G. Devyatkov, Zh. Eksperim. i Teor. Fiz. 47, 1588 (1964) [English transl.: Soviet Phys.—JETP 20, 1067 (1965)].

[2] C. Benoit a la Guillaume and J. M. Debever, Compt. Rend. 261, 5428 (1965).

[3] C. E. Hurwitz, Appl. Phys. Letters 8, 121 (1966).

[4] C. Benoit a la Guillaume and J. M. Debever, Phys. Status Solidi 17, 875 (1966); C. Benoit a la Guillaume, J. M. Debever, and F. Salvan, in *Proceedings of the International Conference on II-VI Semiconducting Compounds, 1967*, edited by D. G. Thomas (W. A. Benjamin, Inc., New York, 1968), p. 669.

[5] L. A. Kulewsky and A. M. Prokhorov, IEEE J. Quantum Electron. QE, 2584 (1966).

(iv) The spectra were measured by means of a logarithmic amplifier in order to reasonably reduce the large variations of the light intensity (more than 100 dB).

III. MEASUREMENT TECHNIQUE OF OPTICAL GAIN

The measurement technique of the optical gain has been described in a previous publication.[4] It consists in comparing the spectra emitted in two directions labeled A and B, which are, respectively, perpendicular and parallel to the excited surface of the sample of (Fig. 1).

The electron-accelerating voltage is 25 kV so that the penetration depth is about 1 μ. The photons emitted in the direction A pass only through a small thickness of the excited material, and the spectrum obtained is due to spontaneous emission. On the other hand, the photons emitted in the direction B can be amplified over a large path, since the spot diameter can vary between 200 μ and some millimeters. In this case, we obtain a stimulated spectrum if the excitation intensity is sufficiently high.

The geometry used here is nonresonant so that the spectrum B is simply the spectrum A amplified along a single path. For the sake of simplicity, let us assume that the electron spot is rectangular of a length l in the B direction, and that the excitation is uniformly distributed over the volume. If $I_A(h\nu)$ is the shape of the spontaneous emission line as a function of energy and $\alpha(h\nu)$ the absorption coefficient, positive or negative for the considered excitation and energy, we obtain

$$I_B(h\nu) = K \int_0^l I_A(h\nu) e^{-\alpha(h\nu)x} dx.$$
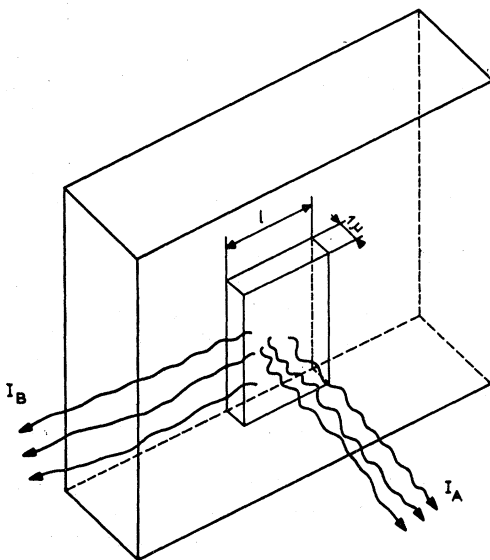
FIG. 1. Disposition of the sample to measure the spontaneous spectrum I_A and the gain (from I_B).

Therefore,

$$I_B(h\nu) = K I_A(h\nu) \frac{1 - e^{-\alpha(h\nu)l}}{\alpha(h\nu) \cdot l}.$$

Experimentally, we obtain $\log I_B(h\nu)$ and $\log I_A(h\nu)$. The previous relation can be written

$$\log \frac{I_B(h\nu)}{I_A(h\nu)} = \log K + \log \left| \frac{1 - e^{-\alpha(h\nu)l}}{\alpha(h\nu)l} \right|.$$

In principle, the absorption coefficient of the non-excited part of the sample situated on the path of the beam must be taken into account. However, in our case the sample is practically transparent in the spectra range studied.

For energies much smaller than the energy of the free exciton, the coefficient of absorption or amplification $\alpha(h\nu)$ is practically zero. The experimental curves $\log I_B(h\nu)$ and $\log I_A(h\nu)$ are thus parallel, and their separation determines $\log K$ (see Fig. 9A).

The absolute value of $\log\{ |e^{-\alpha(h\nu)l} - 1| / |-\alpha(h\nu)| \}$ is obtained from the previous relation. $\alpha(h\nu)$ is then easily determined once l is known.

These results are valid even if the excitation spot is not rectangular, but circular. In this case l, which can be calculated without any difficulty, is of the order of magnitude of the spot diameter. In the high-excitation case some limitations will occur in this treatment and will be discussed in Sec. V.

Our experiments have consisted in studying the time evolution of $\alpha(h\nu) \times l$ as a function of the excitation intensity and of the temperature. It must be noted that our experiments have been realized with different values
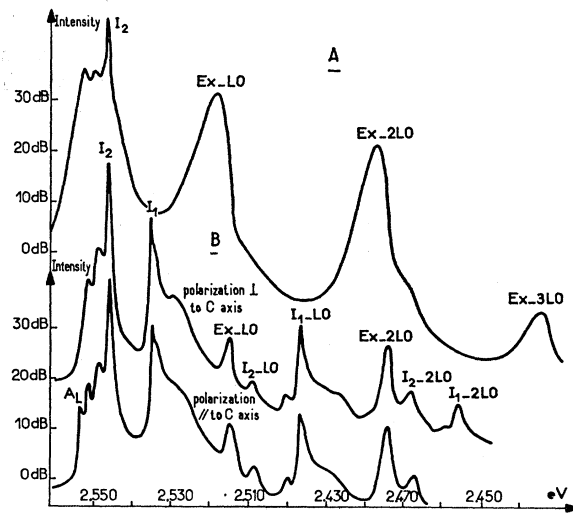
FIG. 2. Spectra of spontaneous emission of CdS at low excitation. Fig. 2(A) shows the fluorescence of a very pure sample at 20°K. Fig. 2(B) shows the spectrum emitted at 8°K by a sample containing the neutral acceptor responsible for the I_1 line and its associates. The ratio of the intensity of the spectra obtained with parallel and perpendicular polarizations is respected.

FIG. 3. Emission lines of CdS and measured separations.

Emission line	Energy eV	Distances between associated lines in meV	Origin
A_L	2.5545		– annihilation of a free exciton in the singlet state (only visible in polarization parallel to the C axis).
$A(1S_T)$	2.5537		– Not observed (see ref. 6).
A_F	2.5525		– Annihilation of a free exciton in the triplet state.
I_2	2.547		– Annihilation of an exciton bound to a neutral donor.
I_1	2.536	40 meV	– Annihilation of an exciton bound to a neutral acceptor.
P	2.527	38 meV	– See the text.
Ex–LO	2.514		– Annihilation of a free exciton with emission of one LO phonon.
I_2–LO	2.509	41 meV 39 meV	– Annihilation of an exciton bound to a neutral donor with emission of one LO phonon.
I_1–LO	2.497	41 meV	– I_1 replica with one LO phonon
Ex–2LO	2.473	41 meV	– Annihilation of a free exciton with emission of two LO phonons.
I_2–2LO	2.468	41 meV	– I_2 replica with two LO phonons.
I_1–2LO	2.456		– I_1 replica with two LO phonons.
Ex–3LO	2.432		– Annihilation of a free exciton with emission of three LO phonons.

of l in order to distinguish the high-gain and also the weak-gain processes. Different types of crystals have been studied.

IV. EXPERIMENTAL RESULTS AND INTERPRETATIONS

A. Spontaneous Emission at Low Excitation

The results obtained are quite similar to those of Thomas and Hopfield.[6,7] They depend very much on the purity of the "platelets" used. Figures 2(A) and 2(B) show the fluorescence spectrum at 20 and 8°K obtained, respectively, with a sample of high purity, and with a sample containing the acceptor responsible for the I_1 line and its associated structure. Figure 3 gives the nature and the position of the emission lines whose origin is understood.

From the measurement of the separation between the lines I_2 and I_2-LO Thomas and Hopfield find that the energy of the LO phonon is 37.7 meV.[7] This value is confirmed by results on the Raman effect in CdS.[8] We find 38 meV for this separation (see Fig. 3), but we obtain 39 meV between I_1 and I_1-LO, and 41 meV for the other processes in which LO phonons are involved.

The position of the lines is determined with an accuracy better than 1 meV, except perhaps for the lines Ex-LO, Ex-2LO, and Ex-3LO at high temperature because of broadening phenomena, which may explain the 40-meV value found between $A(1S_T)$ and Ex-LO.

We therefore believe that the LO phonon energy is 41 meV rather than 37.7 meV. The reason for the discrepancy between I_2, I_2-LO, and I_1-LO is not clearly understood. It is possible that the emitted phonons in these two transitions are not lattice phonons, but localized modes associated with the impurity centers responsible for the I_1 and I_2 lines.

Variable temperature. Figure 4 shows the temperature dependence of the spectrum emitted by CdS at low

[6] J. J. Hopfield and D. G. Thomas, Phys. Rev. **122**, 35 (1961).
[7] D. G. Thomas and J. J. Hopfield, Phys. Rev. **128**, 2135 (1962).
[8] B. Tell, T. C. Damen, and S. P. S. Porto, Phys. Rev. **144**, 771 (1966).
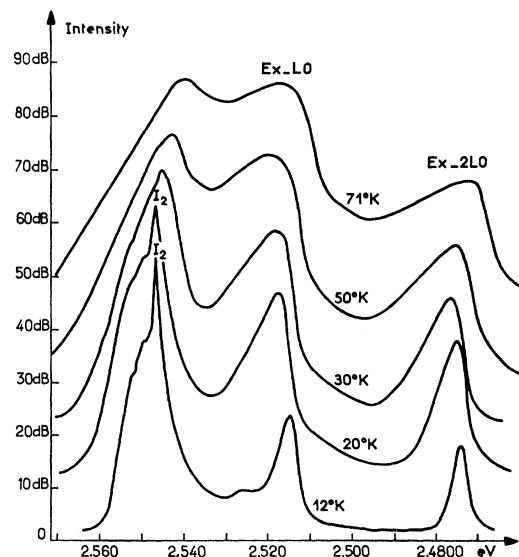
FIG. 4. Spectrum of spontaneous emission of CdS at low excitation for different temperatures. The different spectra have been shifted on the vertical scale by an arbitrary amount.

excitation. Our results confirm and complete those previously obtained.[9]

1. Ex-LO and Ex-2LO Lines

In Figs. 5(A) and 5(B), we have represented the half-widths of the Ex-LO and Ex-2LO lines, and in Fig. 5(C) the ratio of the intensity of the maximum of these two lines, as a function of temperature. It can be seen that both widths vary approximately linearly with temperature, and that the previous ratio begins to saturate at about 50°K.

2. I_2 and I_1 Lines

The spectra represented in Fig. 4 show that the I_2 and I_1 lines vanish, respectively, at approximately 35 and 50°K. These temperatures correspond to values of kT greater than the respective binding energies of excitons to their impurity centers. Therefore, near 50°K, the spectrum is only due to free excitons and the Ex-LO line tends to become as important as the no-phonon one when the temperature is increased.

3. A_L Line

The A_L line which is clearly seen for the polarization parallel to the C axis does not broaden until 50°K. Therefore, this line allows a precise determination of the temperature dependence of the band gap, as shown in Fig. 5(D).

B. Spontaneous Emission at High Excitation

Figure 6 shows the dependence of the spectrum on excitation level. The light intensity is plotted on a logarithmic scale from an arbitrary 0-dB level, which is the same for all our experiments. The current density J increases, in arbitrary units, from 2.5 to 500, which corresponds approximately to 1 A/cm².

The essential feature consists of a very large broadening at high excitation towards the low and also the high energies. This gives a "triangular" aspect to the spectra.

We have studied the kinetics of the different lines as a function of excitation. The weakest excitations are obtained by bombarding the sample with a continuous current smaller than 10^{-9} A. The high excitations are realized by means of 1-μsec or 100-nsec pulses in order to avoid heating effects. There is therefore an unexplored zone between the weak and high excitations, and the kinetics corresponding to these two excitation conditions hardly overlap.
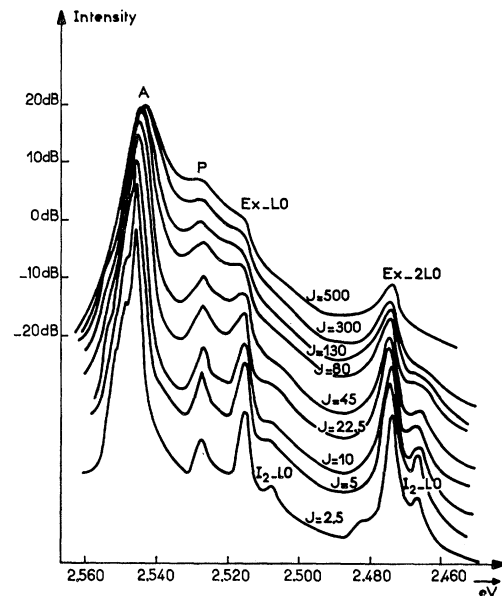
FIG. 6. Spectrum of spontaneous emission of pure CdS at about 10°K as a function of the excitation J. It is given in relative units (from 0.5 to 500). The 0-dB level is arbitrary but common to all spectra.

We obtain the following results as a function of the excitation J:

(i) The Ex-2LO line is proportional to J at low excitation and varies as $J^{1/2}$ at high excitation [Fig. 7(A)]. This line is well separated from the others, and is used to measure (in relative value) the number of free excitons in the system.

(ii) The P line (2.527 meV) which will be discussed ater is not present at low excitation. At higher excitation it increases rapidly, proportional to J, and thus to the square of the number of free excitons [Fig. 7(B)].

FIG. 5. (A) Half-width for the Ex-2LO line, (B) half-width for the Ex-LO line, (C) ratio of the intensities of the Ex-Lo and Ex-2LO lines at their respective maximum, (D) variation of the band gap versus temperature.

[9] E. Gross, S. Permogorov, and B. Razbirin, J. Phys. Chem. Solids **27**, 1647 (1966); C. E. Bleil and J. G. Gay, in *Proceedings of the International Conference on the II–VI Semiconducting Compounds, Providence, 1967*, edited by D. G. Thomas (W. A. Benjamin, Inc., New York, 1968), p. 360; C. E. Bleil and I.

Broser, in *Proceedings of the International Conference on the Physics of Semiconductors, Paris, 1964* (Academic Press Inc., New York, 1965).

(iii) The I_2 line is mixed with a broader one which we call the A line. This line shifts towards low energies when J is increased, and its level becomes progressively saturated.

(iv) The low-energy tail, which is clearly seen between the Ex-LO and Ex-2LO lines, tends to dominate. For the excitations used, its slope is 0.5 dB/meV. The level of this low-energy tail, measured at a given energy between Ex-LO and Ex-2LO, has a variation proportional to J [Fig. 7(C)], and therefore proportional to the square of the exciton number, as in the case of the P line.

To summarize, the bound exciton transitions saturate very rapidly with excitation, and only the transitions related to the free excitons persist. It is worth noting that the spectra emitted at high excitation do not depend on the type of "platelets" used, contrary to the case of those emitted at low excitation.
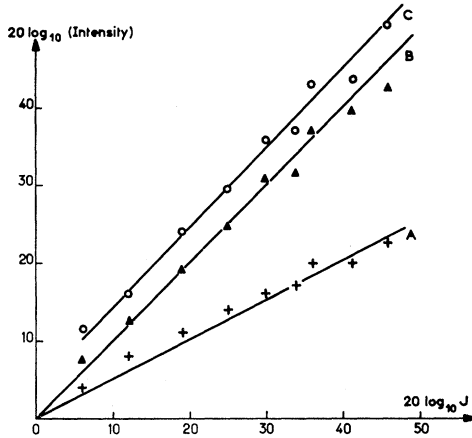
FIG. 7. (A) Kinetics of the Ex-2LO line as a function of J (slope 0.5), (B) kinetics of the P line as a function of J (slope 1), (C) kinetics of the low-energy tail, measured at a given energy between Ex-LO and Ex-2LO as a function of J (slope 1).

1. Time Effects

None of the phenomena which we have described up to now show any time dependence. If the excitation exceeds 3 A/cm², some modifications depending on time appear [Fig. 8(A)]. Let us note that these modifications will be found again in the gain study, but very amplified in this case.

The mean slope of the low-energy tail decreases from 0.5 to 0.3 dB/meV when J increases from 3 to 10 A/cm². This slope decreases slightly with time. The Ex-2LO line which emerges weakly can still be seen.

The high-energy side of the light intensity decreases with time, whereas its low-energy side increases. The A line is merged with a broad line at the beginning of the pulse. This broad line seems to shift towards lower energies, and its intensity decreases at the same time. The A line which reappears 20 nsec after the beginning of the pulse has a maximum whose energy does not
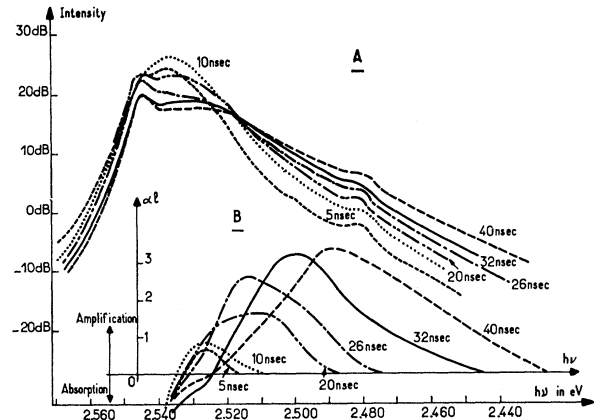
FIG. 8. (A) Variation of the spontaneous spectrum at very high excitation $(J=10$ A/cm²) as a function of the delay after the beginning of the pulse, (B) variation of $\alpha(h\nu)l$ under the same conditions.

vary very much with time. This shows that the crystal-lattice temperature does not increase appreciably with time when the pulses are short, and it is not possible to interpret the gain effects described further as arising from a temperature increase.

C. Gain of the Ex-LO Process

In Fig. 9(A) are shown the spectra $\log_{10} I_A(h\nu)$ and $\log_{10} I_B(h\nu)$ obtained in CdS at 20°K with an excited spot strongly defocused $(l \simeq 1$ mm). Figure 9(B) gives the product $\alpha(h\nu) \times l$ in the case of four increasing excitations.

From Fig. 9(B), it can be seen that at low excitation $(J=5)$ there is an absorption coefficient due to the non-
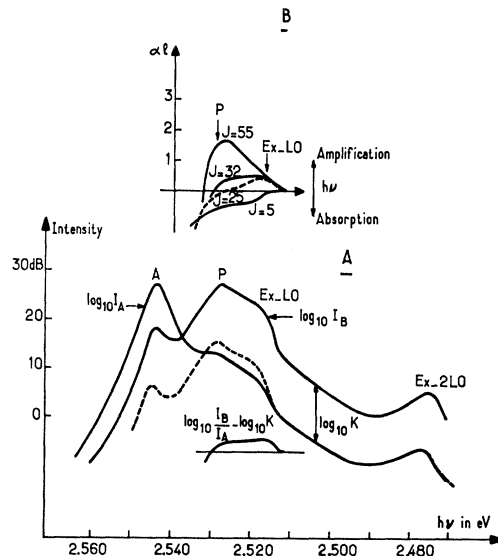
FIG. 9. (A) An example of spectra I_A and I_B just at the onset of amplification. (B) Variation of $\alpha(h\nu)l$ at different excitation. $J=32$ corresponds to about 1 A/cm².

excited material. When the excitation is increased, the gain appears in the Ex-LO line ($J=25$), then it extends to the P line ($J=32$), and finally becomes largely preponderant in the P line ($J=55$). In the excitation condition of Fig. 9(B), for $J=32$, $\alpha(h\nu)$ is at most equal to 0.4, so that $\alpha \simeq 4$ cm^{-1}, since $\simeq 1$ mm.

D. High-Gain Process

We have seen [Fig. 9(B)] that the gain curve is centered on the P line when the excitation is increased. The gain grows with the excitation for values of J ranging from 1 and 3 A/cm^2, but its maximum does not appreciably vary as a function of time.

When $J>3$ A/cm^2, the maximum of the gain curve moves at first slowly towards the low-energy side. Then the amplitude of this displacement grows rapidly with J. Figure 8(B) gives the variation of the gain curve versus time during a 40-nsec pulse, and for an excitation equal to 10 A/cm^2. It can be seen that the corresponding variation of the spontaneous emission is rather small [Fig. 8(A)], so that the increase of the lattice temperature cannot exceed some tens of degrees. The gain variation which is very large (for the highest excitations its maximum can shift by 100 meV between the beginning and the end of the pulse) cannot be attributed to a big variation of the band gap due to a temperature increase, which would have to reach at least 300°K.

When the temperature is increased, the current threshold necessary to obtain some amplification increases slowly and doubles at 77°K. It then grows much more rapidly. The shift effect of the gain curve with time does not seem to be strongly affected by an increase of temperature.

V. THEORY AND INTERPRETATION

We have tried to interpret the modifications of the spontaneous-emission spectrum with excitation and also to find the processes which yield gain. The simplest one is the exciton-LO phonon case which has already been proposed.[5]

In the first part we sketch the theory of this process and we calculate the associated gain.

Besides explaining the very important low-energy tail and the gain which appears at high excitation, it must be noticed that an exciton can be radiatively annihilated only if it loses its momentum either by emitting one or several phonons or by another process. We are going to study two possible mechanisms—the exciton-electron and the exciton-exciton interactions.

A. Exciton-LO Phonon Interaction

An improved treatment of the exciton-LO phonon line shape was published recently.[10] It takes into account

the sum over intermediate states which had not been treated previously.[11]

In fact, all these papers neglect the exciton-photon coupling.[12,13]

Our purpose here is to deduce the number of excitons in the system from a measurement of the amplification coefficient.

Within a small energy range near $h\nu_0$, we can write this amplification coefficient in the form

$$A(h\nu) = C(h\nu - h\nu_0)^{3/2}[n_{\text{ex}} - n_{\text{phonon}}],$$

with

n_{ex}: free exciton density in the corresponding mode,
n_{phonon}: $[1 + \exp(\hbar\omega/kT)]^{-1}$,
$h\nu_0 = E_0 - \hbar\omega$,
E_0: energy of the free exciton near the band extremum,
$\hbar\omega$: energy of the LO phonon;
n_{ex} is given by

$$n_{\text{ex}} = N_0 \exp[-(h\nu - h\nu_0)/kT],$$

where N_0 is the free-exciton density at the band extremum.

The experimental results given in[11] allows us to obtain the value of C:

$$C \simeq 236 \text{ cm}^{-1}(\text{meV})^{-3/2}.$$

Thus,

$$A(h\nu) = C(h\nu - h\nu_0)^{3/2}N_0 \exp[-(h\nu - h\nu_0)/kT],$$

$A(h\nu)$ is maximum for $h\nu - h\nu_0 = \frac{3}{2}kT$.

If we introduce the total number of free excitons at temperature T, which is given by

$$N_{\text{ex}} = N_0(2\pi MkT/h^2)^{3/2},$$

we thus get for A_{max}:

$$A_{\text{max}} = CN_{\text{ex}} \exp(-\tfrac{3}{2})(3\pi\hbar^2/M)^{3/2}.$$

The following numerical values can be deduced:

$$A_{\text{max}} = 0.4 \cdot 10^{-15}N_{\text{ex}},$$

where A_{max} is in cm^{-1} and N_{ex} is in cm^{-3}. The gain that we have determined depends only on the total number of excitons and not on temperature. In the excitation conditions of Fig. 9(B) ($J=32$):

$$A_{\text{max}} = 4 \text{ cm}^{-1}.$$

Therefore,

$$N_{\text{ex}} = 10^{16} \text{ cm}^{-3}.$$

Since the Ex-2LO line is proportional to N_{ex}, the calibration may be done at this point, so that it is possible to know N_{ex} in absolute value as a function of the excitation.

[10] G. D. Mahan and B. Segall, in *Proceedings of the International Conference on the II-VI Semiconducting Compounds, Providence, 1967*, edited by D. G. Thomas (W. A. Benjamin, Inc., New York, 1968), p. 349.

[11] D. G. Thomas, J. J. Hopfield, and M. Power, Phys. Rev. **119**, 570 (1960).
[12] J. J. Hopfield, Phys. Rev. **112**, 1555 (1958).
[13] W. C. Tait, D. A. Campbell, J. R. Packard, and R. L. Weiher, in *Proceedings of the International Conference on the II-VI Semiconducting Compounds, Providence, 1967*, edited by D. G. Thomas (W. A. Benjamin, Inc., New York, 1968), p. 370.

As mentioned above, the expressions used are valid only for $h\nu - h\nu_0 \ll E_L$, the binding energy of the exciton.

The above theory describes fairly well the experimental situation up to 40°K. Within this range of temperature, we expect from the simplest perturbation theory calculations[11,14] a $3kT$ half-width for the Ex-LO line and also the ratio of the intensities of the maximas of these two lines to be proportional to the temperature.

These three quantities are plotted in Fig. 5. In fact, the experimental results give $2.8kT$ and $4kT$. The ratio of the intensities of the maximas of the two lines behaves as expected.

B. Exciton-Exciton Interaction

Introduction

We first consider a process of exciton-exciton interaction (Fig. 10) which can be described as follows:

Exciton K+Exciton $K' \rightarrow$ Exciton $(K+K')$

$+$ Exciton $0 \rightarrow$ Exciton $(K+K')$+photon $h\nu$.
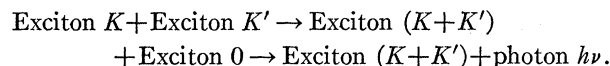
Since the excitons have a Boltzmann distribution at temperature T, the low-energy tail resulting from this process extends only over 2 or $3kT$. Therefore, this process cannot explain our experiments.

The existence of the P line, situated at 2.527 eV, (i.e., 27 meV below the free-exciton level), suggests the following process[15]:

Exciton K+Exciton $K' \rightarrow$ Exciton 0+electron-hole

pair $\rightarrow h\nu$+electron-hole pair.
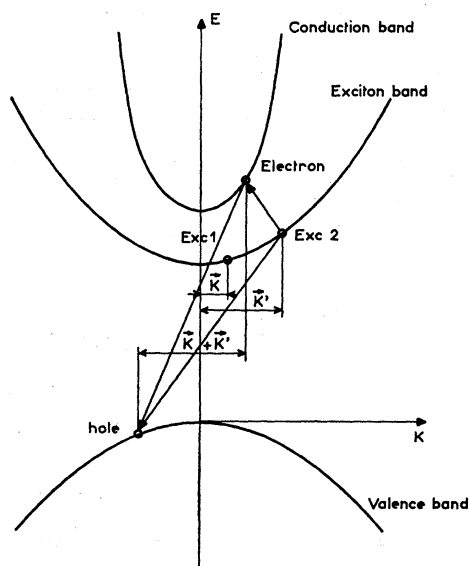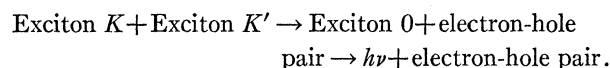
FIG. 10. Sketch of the radiative recombination due to the exciton-exciton interaction.

[14] Y. Toyozawa, Progr. Theoret. Phys. (Kyoto) **20**, 53 (1958).
[15] J. R. Haynes, Phys. Rev. Letters **17**, 866 (1966).

TABLE I. Wave vectors of the particles involved in the exciton-exciton interaction, and energies of the states.

	Initial state	Intermediate state	Final state
Exciton	$\mathbf{K}, \mathbf{K}' \simeq 0$	0	
Electron		$\mathbf{k}_i + \mathbf{K} + \mathbf{K}' \simeq \mathbf{k}_i$	$\mathbf{k}_i$
Hole		$-\mathbf{k}_i$	$-\mathbf{k}_i$
Photon			$h\nu$
Energies	$2E_0 + E_K + E_{K'}$	$E_0 + E_G + (\hbar^2 k_i^2/2\mu)$	$h\nu + E_G + (\hbar^2 k_i^2/2\mu)$

This process, which involves a great number of particles, is difficult to calculate. The situation can be simplified by considering excitons having a momentum almost equal to zero. In this case, the momentum of the electron-hole pairs must be zero.

In Table I, one can see the wave vectors of the particles involved and the energies of the different states.

Here E_K and $E_{K'}$ are the kinetic energies of the excitons, E_G is the band gap and μ is given by $\mu^{-1} = m_e^{-1} + m_h^{-1}$, where m_e, m_h are the electron and hole masses, supposed isotropic for the sake of simplicity.

Using $E_G - E_0 = E_L$ the energy conservation condition may be written as

$$h\nu = E_0 - E_L - \hbar^2 k_i^2/2\mu + E_K + E_{K'}$$

and appears in the calculation of the line shape through the factor

$$\delta(E_0 - E_L - h\nu - \hbar^2 k_i^2/2\mu + E_K + E_{K'}).$$

One therefore expects a line whose position corresponds roughly to the P line. We expect also a low-energy tail for the corresponding line.

It is impossible at this stage to give theoretical calculations of the corresponding line shape. This process involves many particles and is difficult to evaluate.

The probability of a photon emission when two excitons K, K' collide is given by

$$P_E \propto |1 + N(h\nu)| n_K n_{K'} (1 - n_e)(1 - n_h), \quad (1)$$

where $N(h\nu)$, n_K, $n_{K'}$, n_e, n_h are the occupation probabilities of the photon, exciton, electron, and hole in their respective states. We use the fact that n_K, $n_{K'}$, n_e, $n_h \ll 1$, and obtain for the spontaneous process

$$P_{\text{S.E.}} \propto n_K n_{K'}. \quad (2)$$

Absorption being proportional to

$$N(h\nu)(1 + n_K)(1 + n_{K'}) n_e n_h,$$

the difference between stimulated emission and absorption can be shown to be

$$P_G \propto N(h\nu)(n_K n_{K'} - n_e n_h). \quad (3)$$

Since n_K, $n_{K'} \gg n_e n_h$ we expect essentially the same shape for the spontaneous emission and gain curves.

C. Exciton-Electron Interaction

A somewhat similar process was investigated[16] to explain the absorption of photons with energies smaller than the band gap in band to band transitions. We consider Boltzmann distributions of interacting excitons and electrons at temperatures T and T_e. Here T_e can be greater than T because with our excitation method we create hot carriers.

We derive the line shape due to the radiative annihilation of excitons, whose mechanism is illustrated in Fig. 11. We use second-order perturbation theory. The momenta of the particles are shown in Table II.

The total emission probability is

$$P_E \propto [1 + N(h\nu)] n_K n_{k_i} (1 - n_{k_f}). \qquad (4)$$

With the approximation used in Sec. V B this gives for the spontaneous emission

$$P_{\text{S.E.}} \propto n_K n_{k_i}. \qquad (5)$$

The absorption is proportional to

$$N(h\nu)(n_K + 1)(1 - n_{k_i}) n_{k_f}$$

and the net rate of stimulated emission (stimulated emission-absorption) is

$$P_G \propto n_K (n_{k_i} - n_{k_f}) - n_{k_f}. \qquad (6)$$

Let us denote by U_{if} the probability amplitude for a photon to be emitted from an initial $|1s,\mathbf{K}\rangle|\mathbf{k}_i\rangle$ containing one exciton in the $1s$ state and one $\mathbf{k}_i$ electron. The electron which remains in the final state has a wave vector $\mathbf{k}_f$.
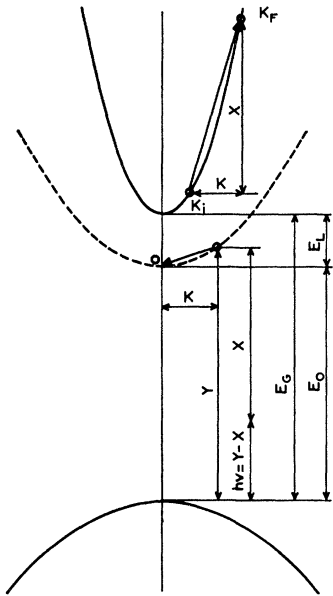
FIG. 11. Sketch of the radiative recombination of an exciton giving its momentum to a free electron.

[16] A. A. Grinberg, N. I. Kramer, A. A. Rogachev, and S. M. Ryvkin, J. Phys. Soc. Japan, Suppl. **21**, 95 (1966).

1. Calculation of U_{if}

A rigorous calculation of U_{if} in our approximation involves a summation over all intermediate states. In order to gain insight into the results we only consider the $1s$ intermediate state. Thus,

$$U_{if} \propto \frac{\langle h\nu | H_{er} | 1s,0\rangle\langle \mathbf{k}_f | \langle 1s,0 | H_{\text{Coul}} | 1s,\mathbf{K}\rangle | \mathbf{k}_i\rangle}{\Delta E}, \qquad (7)$$

where

$H_{\text{Coul}} =$ Coulomb perturbation Hamiltonian,
$H_{er} =$ exciton-photon Hamiltonian,
$\mathbf{k}_i, \mathbf{k}_f =$ wave vectors of the initial, final electron states,
$1s, \mathbf{K} = 1s$ exciton state with a $\mathbf{K}$ wave vector,
$\Delta E =$ energy difference between the initial and intermediate states.

If $M = m_e + m_h$ is the effective mass of the exciton, the different state energies are

initial state:

$$E_0 + \hbar^2 K^2/2M + E_G + \hbar^2 k_i^2/2m_e,$$

intermediate state:

$$E_0 + E_G + \hbar^2 k_f^2/2m_e,$$

final state:

$$h\nu + E_G + \hbar^2 k_f^2/2m_e.$$

From energy conservation $\Delta E = E_0 - h\nu$. We now calculate the matrix element of the Coulomb interaction.

2. Exciton-Electron Scattering

The Hamiltonian of the three-particle system is

$$-\frac{\hbar^2}{2m_e}\Delta_1 - \frac{\hbar^2}{2m_e}\Delta_2 - \frac{\hbar^2}{2m_h}\Delta_h + \frac{e^2}{\epsilon}\left(\frac{1}{r_{12}} - \frac{1}{r_{1h}} - \frac{1}{r_{2h}}\right), \qquad (8)$$

where $r_{ij} = |\mathbf{r}_i - \mathbf{r}_j|$. If we take into account the antisymmetrization with respect to the electrons (1 and 2) the wave function of the unperturbed initial state can be written

$$(1/\sqrt{2}\Omega)[\exp\{i(\mathbf{K}\cdot\mathbf{R}_1 + \mathbf{k}_i\cdot\mathbf{r}_2)\}\phi_{1s}(r_{1h})$$
$$- \exp\{i(\mathbf{K}\cdot\mathbf{R}_2 + \mathbf{k}_i\cdot\mathbf{r}_1)\}\phi_{1s}(r_{2h})], \qquad (9)$$

where $\mathbf{R}_i = (m_e\mathbf{r}_i + m_h\mathbf{r}_h)/M$ and Ω is the volume of the crystal. The perturbing terms for the wave functions

TABLE II. Wave vectors of the particles involved in the exciton-electron interaction.

	Initial state	Intermediate state	Final state
Exciton	$1s, \mathbf{K}$	$ns, \mathbf{K}=0$	
Electron	$\mathbf{k}_i$	$\mathbf{k}_f = \mathbf{k}_i + \mathbf{K}$	$\mathbf{k}_f = \mathbf{k}_i + \mathbf{K}$
Photon			$h\nu$

of (9) are, respectively,

$$\frac{e^2}{\epsilon}\left(\frac{1}{r_{12}}-\frac{1}{r_{2h}}\right) \tag{10}$$

for the first part of the wave function, and

$$\frac{e^2}{\epsilon}\left(\frac{1}{r_{12}}-\frac{1}{r_{1h}}\right) \tag{11}$$

for the second one. The wave function associated with $\langle 1s,0|\langle \mathbf{k}_f|$ is

$$(1/\sqrt{2}\Omega)[\exp\{-i(\mathbf{k}_f\cdot\mathbf{r}_2)\}\phi_{1s}(r_{1h})$$
$$-\exp\{-i(\mathbf{k}_f\cdot\mathbf{r}_1)\}\phi_{1s}(r_{2h})]. \tag{12}$$

The matrix element of (10) and (11) between the corresponding parts of (9) and (12) gives four terms:

(a) direct electron-electron repulsion,

$$e^2/\epsilon\Omega^2\langle\exp(i\mathbf{k}_f\cdot\mathbf{r}_2)\phi_{1s}(r_{1h})|$$
$$\times 1/r_{12}|\exp\{i(\mathbf{K}\cdot\mathbf{R}_1+\mathbf{k}_i\cdot\mathbf{r}_2)\}\phi_{1s}(r_{1h})\rangle; \tag{13}$$

(b) exchange electron-electron repulsion,

$$-e^2/\epsilon\Omega^2\langle\exp(i\mathbf{k}_f\cdot\mathbf{r}_1)\phi_{1s}(r_{2h})|$$
$$\times 1/r_{12}|\exp\{i(\mathbf{K}\cdot\mathbf{R}_1+\mathbf{k}_i\cdot\mathbf{r}_2)\}\phi_{1s}(r_{1h})\rangle; \tag{14}$$

(c) direct electron-hole attraction,

$$-e^2/\epsilon\Omega^2\langle\exp(i\mathbf{k}_f\cdot\mathbf{r}_2)\phi_{1s}(r_{1h})|$$
$$\times 1/r_{2h}|\exp\{i(\mathbf{K}\cdot\mathbf{R}_1+\mathbf{k}_i\cdot\mathbf{r}_2)\}\phi_{1s}(r_{1h})\rangle; \tag{15}$$

(d) exchange electron-hole attraction,

$$e^2/\epsilon\Omega^2\langle\exp(i\mathbf{k}_f\cdot\mathbf{r}_1)\phi_{1s}(r_{2h})|$$
$$\times 1/r_{2h}|\exp\{i(\mathbf{K}\cdot\mathbf{R}_1+\mathbf{k}_i\cdot\mathbf{r}_2)\}\phi_{1s}(r_{1h})\rangle. \tag{16}$$

If we use $1/r_{12}=(4\pi/\Omega)\sum_q(1/q^2)\exp\{i\mathbf{q}\cdot(\mathbf{r}_2-\mathbf{r}_1)\}$ and 1s hydrogenic wave functions, and if we assume that K is sufficiently small, then

$$\langle\mathbf{k}_f|\langle 1s,0|H_{\mathrm{Coul}}|1s\mathbf{K}\rangle|k_i\rangle$$

can be written

$$\langle k_f|\langle 1s,0|H_{\mathrm{Coul}}|1s,\mathbf{K}\rangle|\mathbf{k}_i\rangle\propto\frac{2\pi a_0^2 e^2}{\Omega\epsilon}\left|\frac{m_e-m_h}{M}\right.$$
$$+(1+k_i^2a_0^2)^{-3}\left(\frac{3}{2}-\frac{5}{3}k_i^2a_0^2-\frac{k_i^4a_0^4}{2}\right)\right|, \tag{17}$$

where the $\mathbf{K}$ dependence of the exchange term has been neglected.

In this perturbation calculation we have not considered the exciton-photon coupling (polaritons) which is treated in Refs. 12 and 13. The main effect of taking it into account is, as shown in Ref. 13, to change the energy denominator $(E_0-h\nu)^2$ of $|U_{if}|^2$ into $(E_0-h\nu)^2+(\pi\gamma/\epsilon)E_0^2$.

For numerical calculations we used a value of $(4\pi\gamma/\epsilon)\simeq 10^{-3}$ taken from Ref. 13.

3. Spontaneous Line

If we include polariton effects by modifying the energy denominator occurring in perturbation theory, we obtain for $P(h\nu)$

$$P_S(h\nu)\frac{N_0n_0|A'|^2}{(E_0-h\nu)^2+(\pi\gamma/\epsilon)E_0^2}\int d^3K d^3k_i$$
$$\times\exp\left\{-\frac{\hbar^2}{2}\left(\frac{K^2}{M}\beta+\frac{k_i^2}{m_e}\beta_e\right)\right\}|U_{if}|^2$$
$$\times\delta\left[E_0-h\nu+\frac{\hbar^2K^2}{2}\left(\frac{1}{M}-\frac{1}{m_e}\right)-\frac{\hbar^2}{m_e}\mathbf{k}_i\mathbf{K}\right]. \tag{18}$$

$|A'|^2$ comes from the optical matrix element and N_0, n_0 are the occupation numbers of excitons and electrons for a null wave vector.

In (18) we may neglect the variation of $|U_{if}|^2$ with $\mathbf{k}_i$ when $k_i^2>2m_e/\beta_e\hbar^2$ because of the occurrence of the exponential term

$$\exp\{-(\hbar^2k_i^2/2m_e)\beta_e\}.$$

By inspection of (17) we see that for $k_i<\frac{1}{2}k_0=(1/2a_0)$ the k_i dependence of U_{if} can be neglected. Thus for $2m_e(\beta_e)^{-1}/\hbar^2<\frac{1}{4}k_0^2$, i.e., $kT_e<\frac{1}{4}E_L$, we can take $|U_{if}|^2$ constant. The $\mathbf{k}_i$ integration is easily evaluated using

$$\int d^3k_i\exp\left\{-\frac{\hbar^2k_i^2}{2m_e}\beta_e\right\}\delta\left[E_0-h\nu+\frac{\hbar^2K^2}{2}\left(\frac{1}{M}-\frac{1}{m_e}\right)-\frac{\hbar^2}{m_e}\mathbf{k}_i\mathbf{K}\right]$$

$$=\int dS_{k_i}\frac{\exp\{-(\hbar^2k_i^2/2m_e)\beta_e\}}{|\mathrm{grad}_{k_i}(E_0-h\nu+\frac{1}{2}\hbar^2K^2[(1/M)-(1/m_e)]-(\hbar^2/m_e)\mathbf{k}_i\mathbf{K}|)}, \tag{19}$$

where the integration must be done on the surface defined by

$$E_0-h\nu+\frac{\hbar^2K^2}{2}\left(\frac{1}{M}-\frac{1}{m_e}\right)-\frac{\hbar^2}{m_e}k_iK=0, \tag{20}$$

which represents a plane perpendicular to $\mathbf{K}$. If we take $\mathbf{K}$ parallel to Oz we finally obtain for (19)

$$\frac{2\pi m_e^2}{\hbar^4 \beta_e}\frac{1}{K}\exp\left\{-\frac{m_e\beta_e}{2\hbar^2 K^2}\right\}\left|E_0-h\nu+\frac{\hbar^2 K^2}{2}\left(\frac{1}{M}-\frac{1}{m_e}\right)\right|^2.$$

After some calculations $P_S(h\nu)$ is found to be

$$P_S(h\nu)\propto\frac{N_0 n_0}{(E_0-h\nu)^2+(\pi\gamma/\epsilon)E_0^2}\frac{1}{\beta_e}\exp\left\{\frac{m_h}{2M}\beta_e(E_0-h\nu)\right\}\int_0^\infty\left(\frac{\alpha_2}{\alpha_1}\right)^{1/2}\exp\left\{(\alpha_1\alpha_2)^{1/2}\left(t+\frac{1}{t}\right)\right\}dt,\qquad(21)$$

where

$$\alpha_1=\frac{\hbar^2\beta_e}{2M}\left|\frac{\beta}{\beta_e}+\frac{m_h^2}{4m_eM}\right|,\qquad\alpha_2=\frac{m_e\beta_e}{2\hbar^2}(E_0-h\nu)^2.$$

From Ref. 17 we evaluate the integral in (21) and we finally obtain

$$P_S(h\nu)\propto\frac{1}{\beta_e}\frac{N_0 n_0}{(E_0-h\nu)^2+(\pi\gamma/\epsilon)E_0^2}\left(\frac{\alpha_2}{\alpha_1}\right)^{1/2}K_1\{2(\alpha_1\alpha_2)^{1/2}\}\exp\left\{\frac{m_h\beta_e}{2M}(E_0-h\nu)\right\},\qquad(22)$$

where $K_1(x)$ is the first-order modified Bessel function of the third kind. The results for the line shape were calculated on a computer.

To perform these calculations N_0 and n_0 have been expressed as a function of the total number of electrons and excitons and their respective temperatures. In addition, we have injected the values of the known parameters[18] in (22): $m_e=0.2m_0$, $m_h=1.4m_0$, $m_0=$ mass of the electron.

4. Gain Curve

With the help of (6) we have calculated the gain curve. We proceed exactly as in Sec. V C 2 and finally obtain

$$P_G(h\nu)\propto\frac{n_0}{\beta_e}\frac{1}{(E_0-h\nu)^2+(\pi\gamma/\epsilon)E_0^2}\left|N_0\left(\frac{\alpha_2}{\alpha_1}\right)^{1/2}K_1\{2(\alpha_1\alpha_2)^{1/2}\}\exp\frac{m_h\beta_e}{2M}(E_0-h\nu)-N_0\left(\frac{\beta_2}{\beta_1}\right)^{1/2}K_1\{2(\beta_1\beta_2)^{1/2}\}\right.$$

$$\left.\times\exp\left\{-\left(1-\frac{m_h}{2M}\right)\beta_e(E_0-h\nu)\right\}-\left(\frac{\gamma_2}{\gamma_1}\right)K_1\{2(\gamma_1\gamma_2)^{1/2}\}\exp\left\{-\left(1-\frac{m_h}{2M}\right)\beta_e(E_0-h\nu)\right\}\right|,\qquad(23)$$

where

$$\alpha_1=\frac{\hbar^2\beta_e}{2M}\left(\frac{\beta}{\beta_e}+\frac{m_h^2}{4m_eM}\right),\qquad\alpha_2=\beta_2=\gamma_2=\frac{m_e}{2\hbar^2}\beta_e(E_0-h\nu)^2,$$

$$\beta_1=\frac{\hbar^2\beta_e}{2M}\left(\frac{\beta}{\beta_e}+\frac{m_h^2}{4m_eM}+1\right),\qquad\gamma_1=\frac{\hbar^2\beta_e}{2M}\left(\frac{m_h^2}{4m_eM}+1\right);$$

(23) was also evaluated by means of a computer. All these results will be discussed below.

D. Kinetics as a Function of the Excitation

If the two preceding processes are taken into account, the kinetics as a function of the excitation may be expressed as follows:

$$dn/dt=J-(A+A')np+\tfrac{1}{2}(C+C')n_{ex}^2,$$

$$dn_{ex}/dt=Anp-n_{ex}/\tau-(B+B')nn_{ex}-(C+C')n_{ex}^2,$$

where n is the electron density, p the hole density and n_{ex} the free exciton density.

In the first equation

$J=$ excitation $=$ electron-hole pair creation,

$(A+A')np=$ electron-hole pair recombination. Anp corresponds to the creation of excitons; and $A'np$ describes the radiative or nonradiative direct recombination,

$\tfrac{1}{2}(C+C')n_{ex}^2=$ number of electron-hole pairs created by the exciton-exciton process,

$n_{ex}/\tau=$ radiative or nonradiative recombination of free excitons whose lifetime is τ,

$(B+B')nn_{ex}=$ exciton-electron process recombination. Bnn_{ex} is the radiative term and $B'nn_{ex}$ the nonradiative one,

$(C+C')n_{ex}^2=$ recombination due to exciton-exciton processes. Cn_{ex}^2 is the radiative term and $C'n_{ex}^2$ is the nonradiative one.

[17] *Tables of Integral Transforms*, edited by A. Erdelyi (McGraw-Hill Book Co., New York, 1953), Vol. 1, p. 146.

[18] R. R. Sharma and S. Rodrigez, Phys. Rev. **153**, 823 (1967).

All the coefficients used may depend on temperature. We shall put $n=p$. In the steady state (in some cases a spike regime has been observed at the beginning of the pulse)

$$\frac{dn}{dt}=\frac{dn_{ex}}{dt}=0.$$

Therefore,

$$J=(A+A')n^2-\tfrac{1}{2}(C+C')n_{ex}^2, \qquad (24)$$

$$An^2=n_{ex}/\tau+(B+B')nn_{ex}+(C+C')n_{ex}^2. \qquad (25)$$

1. Weak Excitation Case

$(B+B')nn_{ex}$ and $(C+C')n_{ex}^2$ are negligible so that

$$J=(A+A')n^2 \quad \text{and} \quad An^2=n_{ex}/\tau,$$

therefore,

$$J=(A+A')n^2=[(A+A')/A\tau]n_{ex}.$$

Subsequently, the free-exciton number is proportional to J and the Ex-2LO line is proportional to the excitation. Let us note that this is experimentally verified. In this case $n_{ex}=\tau An^2$, and it is possible to find an approximate value of A. τ is the exciton lifetime and can be measured from the risetime of the fluorescence light pulses which gives $\tau\sim5$ nsec. An order of magnitude of A can be deduced from the analogy between our problem and the case of the capture of an electron by an ionized donor in silicon. This analogy is justified by taking into account that holes are much heavier than electrons in CdS. The coefficient corresponding to A ranges from 10^{-6} to 10^{-5} in silicon.[19] In fact, the value of A could be different in the case we consider because of a different electron phonon coupling; but n varies as $A^{-1/2}$ and is not very much affected by a variation of this coefficient.

Therefore, $n^2\sim10^{14}n_{ex}$ and, for instance, $n=10^{15}$ when $n_{ex}=10^{16}$ cm^{-3}. This result is quite acceptable and it can be seen that the ratio n^2/n_{ex} is very different from the value obtained at the thermal equilibrium.

2. High-Excitation Case

If $(C+C')n_{ex}^2$ is dominant, it is clear from (25) that the exciton number is proportional to the number of electrons. In this case, (24) shows that the low-energy tail, which is proportional to Cn_{ex}^2 varies as J and the Ex-2LO line which is proportional to n_{ex} has a $J^{1/2}$ variation. The same results are obtained if $(B+B')nn_{ex}$ is dominant.

These dependences are in good agreement with the experiments. The P line attributed here to an exciton-exciton process depends linearly on J, as does the low-energy tail, which may be due to either of the two processes considered. In addition, let us note that the Ex-2LO line has $J^{1/2}$ kinetics (Fig. 7). However, these

kinetics have not been studied for the largest values of the excitation corresponding to the appearance of time effects. In Fig. 7, $J<3$ A/cm^2.

In the case where we have observed a bend of the Ex-2LO line kinetics (transformation of a J dependence to a $J^{1/2}$ dependence), this bend is related to the appearance of the P line.

We have not performed any absolute measurements of the radiative efficiency; and from the spectra represented in Fig. 6, it is difficult to conclude that the radiative terms B or C are more important than B' or C' at medium excitation, in terms of the process considered.

It is possible to consider an efficient nonradiative Auger process involving two excitons, i.e., annihilation of two excitons creating a high-energy electron-hole pair with energy and momentum conservation. However, in the case of an exciton-electron process the Auger effect, where an exciton is annihilated and yields its energy to an electron, is not efficient because the momentum cannot be conserved. Therefore, B' cannot be much greater than B whereas C' can be much more important than C.

Let us finally note that the radiative processes are largely dominant at high excitations and therefore in laser action. However, Eqs. (24) and (25) are only valid when the spontaneous emission is much more important than the induced emission. In the opposite case, recombination terms depending on the photon density in the system must be introduced. For a given excitation density, it is always possible to decrease the importance of the stimulated emission with respect to the spontaneous one by reducing the excitation spot diameter. But this is limited to about 300 μ by our experimental setup. With this minimum value of the spot diameter, the stimulated emission becomes important for $J>3$ A/cm^2. For this reason, the experimental study of the kinetics has not been made for higher values of J.

For $J>3$ A/cm^3, the stimulated emission is all important since all the light is practically emitted in the sample plane $(I_B>I_A)$. In this case it may be assumed that the radiative efficiency is nearly equal to 1. Equations (24) and (25) must therefore be modified to take into account the influence of the stimulated emission and the fact that the energy of the initial electron-hole pair is entirely converted into light.

E. Interpretation

It is thought that the three processes which have been considered here can give a good account of the excitation dependence of the spontaneous emission and of the gain.

1. For $J<1A/cm^2$

Only the Ex-LO process yields some gain. This gain, proportional to n_{ex}, is weak (some cm^{-1}) and requires long cavities to obtain the laser effect. This is the case of Kulewsky and Prokhorov's[5] experiments. However, in our experiments,[4] the cavities used are so short that

[19] M. Loewenstein and A. Honig, Phys. Rev. **144**, 781 (1966).

the gain relative to this transition cannot compensate the losses. This process is particularly interesting because the absolute value of the density of free excitons in the system can be obtained by gain measurements.

2. For $1\ A/cm^2 < J < 3\ A/cm^2$

The gain on the P line becomes dominant. The exciton-exciton interaction is used to explain the position of the line, the existence of a low-energy tail, its kinetics as a function of J and the fact that the gain curve has the same shape as the spontaneous line.

The occurrence of this line at an energy near $E_0 - E_L$ and its kinetics, which varies as n_{ex}^2, provide some support to our interpretation. Calculations giving the shape of the line are planned.

As has been shown, the gain due to this process has the same spectral dependence as the spontaneous emission. For $J = 3$ A/cm², the experiment yields $\alpha_{max}(h\nu) \times l \simeq 3$ so that $\alpha \simeq 20$ cm^{-1} since $l \simeq 0.7$ mm. In this excitation range, the gain obtained is proportional to n_{ex}^2 and is more important than in the case of the Ex-LO process. Large spot diameters are nevertheless required to observe this phenomenon. We think that this process is responsible for the laser effect in medium length cavities (some hundreds of μ).

3. For $J > 3\ A/cm^2$

For $J > 3$ A/cm², time effects appear. As is shown in Fig. 8, they correspond to a small variation of the slope of the low-energy tail during the pulse and to a large shift of the maximum of the gain curve. These experimental facts are interpreted as being manifestations of of the exciton-electron interaction process.

The analysis of the theoretical results obtained in Sec. V C leads to the following deductions:
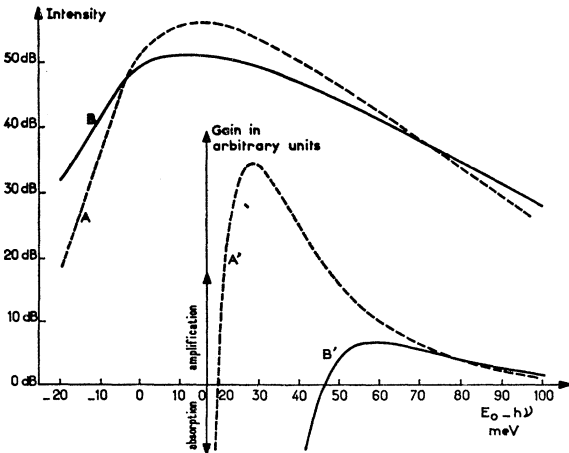
FIG. 12. Theoretical shapes of the spontaneous and gain curves corresponding to the exciton-electron interaction for different values of the parameters:

$-A$ and A':　$kT = 3$ meV,　$kT_e = 4$ meV,　$n_{ex} = 10^{16}$ cm^{-3};
$-B$ and B':　$kT = 4$ meV,　$kT_e = 8$ meV,　$n_{ex} = 10^{16}$ cm^{-3}.

Spontaneous emission. The shape of the spontaneous emission line given by (22) has been calculated for different values of the parameters $\beta = 1/kT$, $\beta_e = 1/kT_e$, n_{ex} (free-exciton density at temperature T) and n_{el} (free-electron density at temperature T_e). The line shape, represented in Fig. 12 for two series of values of the preceding parameters, depends only on β and β_e. The slope of the high-energy tail varies with β_e, but not with the other parameters whereas the slope of the low-energy tail is mainly fixed by β because the influence of β_e is rather weak. This last result may be understood by considering an approximate line-shape formula which is obtained by taking $K_1(x) = (\pi/2x)^{1/2}e^{-x}$ in (22) for $h\nu \ll E_0$.

In this case, we obtain

$$P_S(h\nu) \propto \frac{(E_0 - h\nu)^{1/2}}{(E_0 - h\nu)^2 + (\pi\gamma/\epsilon)E_0^2}$$

$$\times \exp\left\{ -\frac{(E_0 - h\nu)\beta e}{2M}\left[\left(4m_e M \frac{\beta}{\beta_e} + m_h^2\right)^{1/2} - m_h\right]\right\}.$$

The $h\nu$ variation of the term which multiplies the exponential is not very important, and the slope of the low-energy tail is approximately equal to

$$-(20\ \log_{10}e)\frac{\beta_e}{2M}\left[\left(4m_e M\frac{\beta}{\beta_e} + m_h^2\right)^{1/2} - m_h\right]\ \text{in dB/meV}.$$

For example, when $\beta_e = \beta$, the slope given by the previous expression is $-1.1/kT$ dB/meV. For $kT = 2$ meV, this corresponds to the slope due to the exciton exciton process.

Gain. The shape of the gain curve and the position of its maximum depend explicitly on the density of excitons n_{ex} on T, and on T_e, as can be seen in (23).

The variation of the gain amplitude with these three parameters is large and proportional to the electron density n_{el}. In Fig. 12, we have represented the gain curves A' and B' corresponding to the spontaneous emission curves A and B. A systematic study of these curves leads to the following results:

The maximum of the gain curve moves rapidly towards lower energy when T_e and T increase and when n_{ex} decreases. This shift can reach 100 meV for exciton and electron temperatures not greater than 77°K.

We have compared the theoretical and experimental results by taking into account the following considerations:

(a) The phenomena occurring in the high-energy side of the spectra represented in Fig. 8 ($h\nu > 2520$ eV) are difficult to interpret because they may be due to the superposition of several processes chosen among those studied here or even among other ones such as the exciton-exciton interaction (without creation of electron-hole pairs) and the exciton-hole interaction. It is,

however, easy to be convinced that all these processes can be associated with low-energy tails whose slopes are approximately $-1/kT$. If we take into account the scale used for the light intensity, this slope is $[-(20 \log_{10}e)/kT]$ dB/meV, i.e., approximately ten times the slope corresponding to the exciton-electron process. For $h\nu < 2.520$ eV, it is therefore clear that the only processes which may occur at low temperature are those which have been considered in Secs. V B and V C. In addition the variation of the slope of the low-energy tail which varies from 0.5 dB/meV to 0.3 dB/meV when J varies from 3 A/cm² to 10 A/cm² cannot come from another process than the exciton-electron one. For this reason, the comparison between the theoretical and experimental results has only been achieved for $h\nu < 2.520$ eV in the case of the spontaneous emission. As regards the gain curves of Fig. 8(B) corresponding to 5 nsec and 10 nsec, it is difficult to know if they are due to the exciton-exciton process or to the exciton-electron one. Subsequently, only the last four curves have been taken into account.

(b) The measurement method of the optical gain which has been presented in Sec. III is strictly valid only if the stimulated emission is weaker than the spontaneous one. In the opposite case, it is not possible to neglect the influence of the photon density on the de-excitation of the system. If we consider a long rectangular pumped zone in the sample and a constant amplification coefficient $\alpha(h\nu)$ in this region, the treatment of the Sec. III shows that the density of photons due to induced emission at the boundaries of the rectangle will be much greater than the density existing at the center for sufficiently high $\alpha(h\nu)$. When the stimulated emission is the dominant recombination, it follows that the spatial distribution of the excitons and electrons is inhomogeneous since the pumping is uniformly distributed, which is inconsistent with the assumption of a constant gain.

For $J > 3$ A/cm², it is therefore possible that $\alpha(h\nu)$ varies with x, and the experimentally measured amplification coefficient can no longer be simply interpreted. However, if the radiative efficiency is smaller than for these values of J, the nonradiative phenomena are responsible for the variation of the different populations, and not the induced emission. In these conditions, the previous theory remains valid.

In spite of the preceding limitation, we have taken $\alpha(h\nu)$ constant in the excited region of the sample so that the experimental situation represented in Fig. 8 can be described with the following variations of the parameters during the pulse:

beginning of the pulse:

$T = 30°K$, $T_e = 40°K$, $n_{ex} = 10^{16}$ cm⁻³, n_{el} cm⁻³,

end of the pulse:

$T = 40°K$, $T_e = 80°K$, $n_{ex} = 10^{16}$ cm⁻³, $3n_{el}$ cm⁻³.

The values of T are given by the low-energy slope of the spontaneous-emission line, and those of T_e by the position of the maximum of the gain curve. The constant value of n_{ex} is fixed by the constancy of the amplitude of the Ex-2LO line during the pulse. The 10-dB increase of the level of the low-energy tail in spontaneous emission between the beginning and the end of the pulse implies that n_e increases by a factor of 3. With this choice of parameters, the results of Fig. 12 must be raised by 10 dB, and those of Fig. 12(B') must be multiplied by 3. In these conditions, the gain relative to Fig. 8(B) is increased by a factor 2 between 20 nsec and 40 nsec, whereas it is decreased by a factor 2 in Fig. 12. In spite of this discrepancy of a factor of 4 on the gain amplitude, it is satisfying to be able to explain a large shift of its maximum by a weak variation of T and T_e.

The calculation of (23) has been performed for $n_{ex} = 10^{15}$, 10^{16}, 10^{17} cm⁻³. To account for the experimental results, we have chosen $n_{ex} = 10^{16}$ cm⁻³ because $n_{ex} = 10^{17}$ cm⁻³ leads to insufficient displacements of the gain curve and $n_{ex} = 10^{15}$ cm⁻³ to gains whose amplitude is too small. Moreover, it is known from Sec. V A that $n_{ex} \simeq 10^{16}$ cm⁻³ for $J = 1$ A/cm². Subsequently, for $J = 10$ A/cm², values of $n_{ex} \simeq 10^{16}$ cm⁻³ may be expected. The previous calculation would still yield a reasonable result for $n_{ex} = 3 \times 10^{16}$ cm⁻³.

In the high-excitation range, Eqs. (24) and (25) may be written $J = An^2 - \eta R(n_{ex}) = R(n_{ex})$, where $R(n_{ex})$ is the total recombination of excitons (including stimulation) and $\eta = \frac{1}{2}(R_{ex-ex}/R(n_{ex}))$ takes into account the part of $R(n_{ex})$ corresponding to the exciton-exciton process. η is probably always much less than $\frac{1}{2}$, so that $n^2 = (1/A)(1+\eta)J$ increases monotonically with J, but n_{ex}, related to J by $R(n_{ex}) = J$, saturates as a function of J because of the increasing part of the stimulated processes in $R(n_{ex})$. The saturation of n_{ex} probably occurs around 3 A/cm² at a level in the range 1 to 3×10^{16} cm⁻³, whereas n is still increasing. This fact explains why the exciton-electron process overwhelms the exciton-exciton one as J is increased.

An explanation of the large variation of both the free-electron temperature and density during the pulse is required. This may be due to the temperature dependence of the coefficients introduced in Eqs. (24) and (25) particularly in the case of the coefficient A. At the present time, an experiment on the conductivity under excitation is being done in our laboratory. This will allow us to obtain some information relative to the free-electron density and its variation during the pulse.

The experimental results obtained at 77°K with a high excitation are also well explained by this process. To conclude, it is worth noticing that we have measured gains up to 300 cm⁻¹ which may therefore lead to laser action in short cavities.

VI. CONCLUSION

The measurement method of the optical gain allowed us to distinguish three processes able to provide gain in CdS. The best understood one is due to the annihilation of a free exciton with the emission of an optical phonon and the two other processes are related to interactions between excitons and electrons. The transitions related to bound excitons do not occur in our experiments since the results obtained do not depend on the existence of the I_1 line. In spite of the approximations used in the theoretical treatment and the limitations of the experimental interpretation, we think that we have clearly identified the processes responsible for the laser effect in intrinsic CdS. In addition, we want to point out that the results obtained by some authors[20,21] seem to show that the extrinsic process is more efficient than the intrinsic ones to obtain amplification at low injection level.

[20] C. E. Hurwitz, Appl. Phys. Letters **9**, 420 (1966).
[21] C. W. Litton and D. C. Reynolds, in *Proceedings of the International Conference of II-VI Semiconducting Compounds, Providence, 1967*, edited by D. G. Thomas (W. A. Benjamin, Inc., New York, 1968), p. 694.

Backward Stimulated Raman Scattering*

M. Maier and W. Kaiser

Physik-Department der Technischen Hochschule, Munich, Germany

AND

J. A. Giordmaine

Bell Telephone Laboratories, Murray Hill, New Jersey 07974

(Received 26 August 1968)

This paper describes in detail the initiation and growth of backward-traveling stimulated Raman-Stokes pulses. The radiation-transfer equations for the pulse development are derived, and a general analytic solution is given in the rate-equation approximation. Special solutions are given for a variety of pulse-initiation conditions. It is shown that in the presence of residual linear absorption, a steady-state Stokes pulse is expected, and its characteristics are described. Extensive experimental observations in CS₂ of the properties of the backward pulse and the forward emission are reported, including measurements of the pulse energy as a function of position in the cell, the pulse duration as measured by the intensity-autocorrelation technique, and the time sequence of the emission of the forward and backward pulses. Various experimental results indicate the dominant role played by self-focusing in the initiation of the backward pulse and the role of competing processes. The growth of the pulse energy is found to be consistent with the theory; a minimum pulse duration of 30 psec and a peak pulse power 20 times the instantaneous laser pump power are reported, indicating substantial depletion of the incident laser pump light.

I. INTRODUCTION

SINCE the first observations of stimulated Raman scattering,[1,2] backward stimulated Stokes emission and the backward/forward intensity ratio r have remained relatively poorly understood. The theory of stimulated Raman scattering[3-6] shows that under steady-state conditions in the absence of feedback, r should be unity, irrespective of the degree of saturation of the stimulating pump light. Measurements in liquids such as CS₂[7,8] and benzene[9] generally show r in the range 0 to 0.5. Furthermore, the time dependence of the backward emission has been shown in deuterium[10] and H₂ gas[11] to have complex transient behavior on a nanosecond time scale quite different than the forward behavior.

[1] E. J. Woodbury and W. K. Ng, Proc. IRE **50**, 2347 (1962).
[2] G. Eckhardt, R. W. Hellwarth, F. J. McClung, S. E. Schwarz, D. Weiner, and E. J. Woodbury, Phys. Rev. Letters **9**, 455 (1962).
[3] R. W. Hellwarth, Phys. Rev. **130**, 1850 (1963).
[4] E. Garmire, E. Pandarese, and C. H. Townes, Phys. Rev. Letters **11**, 160 (1963).
[5] Y. R. Shen and N. Bloembergen, Phys. Rev. **137**, 1787 (1965).
[6] V. T. Platonenko and R. V. Khokhlov, Zh. Eksperim. i Teor. Fiz. **46**, 560 (1964) [English transl.: Soviet Phys.—JETP **19**, 378 (1964)].

[7] B. P. Stoicheff, Phys. Letters **7**, 186 (1963).
[8] G. Bret and G. Mayer, in *Physics of Quantum Electronics*, edited by P. L. Kelley, B. Lax, and P. E. Tannenwald (McGraw-Hill Book Co., New York, 1966).
[9] P. D. Maker and R. W. Terhune, Phys. Rev. **137**, A801 (1965).
[10] R. W. Minck, E. E. Hagenlocker, and W. G. Rado, Phys. Rev. Letters **17**, 229 (1966); J. Appl. Phys. **38**, 2254 (1967).
[11] W. H. Culver, J. T. A. Vanderslice, and V. W. T. Townsend, Appl. Phys. Letters **12**, 189 (1968).